Thermochimica Acta, 196 (1992) 203–211
Elsevier Science Publishers B.V., Amsterdam

Thermochemical study of gamma bismuth oxide based single crystals

G.S. Suleimenova and V.M. Skorikov

Kurnakov Institute of General and Inorganic Chemistry, USSR Academy of Sciences, Moscow (USSR)

(Received 24 April 1991)

Abstract

The specific heat of $Bi_{12}M_xO_{20-y}$ (M = Si, Ge, Ti, Ga, Fe, Zn; $x \leq 1$; $0 \leq y \leq 0.7$) single crystals has been determined by experimental data obtained using a DSC instrument in the temperature range 50–950 °C. The measurements were conducted on the single crystal specimens at a heating rate of 20 °C min^{-1} in air. The use of the DSC technique provided an insight into a scattering of the specific heat curves of bismuth germanate and silicate samples due to the changes in the electronic contribution in the specific heat related to the defect structure. Changes in the specific heat of the crystal specimens treated in atmospheres with different oxygen partial pressures were detected.

It has been determined that inclusions of a metastable δ^*-phase Bi_2O_3 were due to an exothermal effect at 250–350 °C.

INTRODUCTION

Bismuth trioxide is known to exist in two stable forms: low-temperature α-Bi_2O_3 and high-temperature δ-Bi_2O_3 [1,2]. Two metastable modifications β- and γ-Bi_2O_3 occur in a narrow temperature range during the cooling of δ-Bi_2O_3 to α-Bi_2O_3. The body-centred cubic γ-form of bismuth trioxide is believed to be stabilised by impurities to room temperature.

This paper deals with the thermochemical study of $Bi_{12}M_xO_{20-y}$ (M = Si, Ge, Ga, Fe, Zn; $x \leq 1$; $y < 0.7$) single crystals, a family of stable components with so-called sillenite-type structures related to that of γ-Bi_2O_3.

The single crystals of bismuth germanate, silicate and titanate are piezoelectric, optically active, photoconductive and manifest a linear electro-optic effect [3,4]. Because of their properties, these crystals are of great practical importance. They are used in optical image storage and some other devices.

Pure and mixed bismuth trioxide have been studied by various investigators [5,6], but very little research work has been reported on their thermodynamic properties or, in particular, on the specific heat of $Bi_{12}MO_{20}$ [3] containing various lattice metals.

TABLE 1
The crystallochemical formula, unit cell parameter and temperature of melting or decomposition

Compound	Crystallochemical formula $Bi_{12}(Bi_xM_{1-x})O_{20-y}$ [9]	Unit cell parameter (Å) [9]	Melting character	Melt./decomp. temp., (present paper) (°C)
$Bi_{12}GeO_{20}$	$Bi_{12}(Ge)O$	10.153(4)	Congruent	920.5
$Bi_{12}SiO_{20}$	$Bi_{12}(Si)O_{20}$	10.098	Congruent	893.3
$Bi_{12}TiO_{20}$	$Bi_{12}(Ti_{0.90}\square_{0.10})O_{19.80}$	10.186(3)	Incongruent	857.8
$Bi_{25}GaO_{39}$	$Bi_{12}(Bi_{0.50}Ga_{0.50})O_{19.50}$	10.183(3)	Incongruent	801.7
$Bi_{25}FeO_{39}$	$Bi_{12}(Bi_{0.50}Fe_{0.50})O_{19.50}$	10.184(9)	Incongruent	774.4
$Bi_{38}ZnO_{58}$	$Bi_{12}(Bi_{0.67}Zn_{0.33})O_{19.33}$	10.207(3)	Incongruent	738.9

The sillenite-type crystal structure belongs to the cubic point group 123 [7]. The unit cell is body-centred with MO_4 tetrahedra in the centre and on the top. The tetrahedra are bonded by dimers of (BiO_5) polyhedra, which form the framework of the sillenite structure.

In a recent neutron diffraction study [8,9], $Bi_{12}GeO_{20}$ and $Bi_{12}SiO_{20}$ were recognized as having the ideal sillenite-type structure. The crystallochemical formulae of the compounds studied are given in Table 1, with the tetrahedral sites in parentheses.

As shown in Table 1, $Bi_{12}TiO_{20}$ has approximately 10% of titanium vacancies in tetrahedral sites. For bismuth ferrate, gallate and zincate crystals, the substitution of tetrahedral cations with bismuth cations results in tetrahedra distortion and the loss of one oxygen atom per bismuth atom from the crystal lattice. Therefore, the structures of bismuth ferrate, gallate and zincate are considered to be intermediate between those of bismuth germanate and the so-called "pure" γ-Bi_2O_3.

The present paper gives the results of the specific heat measurements obtained by DSC calorimetry. Moreover, a correlation between the specific heat values obtained and the photoconductive properties [4] of photorefractive sillenite-type crystals is demonstrated. According to refs. 4 and 10, the high photosensitivity of $Bi_{12}MO_{20}$ (M = Si, Ge, Ti) in the visible range of the spectrum is provided by the deep electronic level (E = 2.6 eV) in the forbidden gap (E = 3.5 eV), occurring as a consequence of peculiarities in the defect structure. Changes in the specific heats of crystals resulting from changes in composition have been detected.

EXPERIMENTAL

The single crystals of $Bi_{12}M_xO_{20-y}$ for DSC measurements were provided by V.V. Volkov (Kurnakov Institute of General and Inorganic Chemistry, USSR Academy of Sciences). The starting materials were the oxides

Bi_2O_3, GeO_2, TiO_2, Ga_2O_3, Fe_2O_3 and ZnO, all of high purity (99.99%). For $Bi_{12}GeO_{20}$ and $Bi_{12}SiO_{20}$ crystallisation, the reactants were mixed in stoichiometric ratio (6 : 1). Incongruently melting crystals were grown from the solution in the melt, with Bi_2O_3 added in excess according to phase diagram.

The samples for measurements were obtained by cutting disc specimens from the crystal about 1 mm thick and 5 mm in diameter; the sample weight varied from 170 to 300 mg.

A Netzsch high-temperature DSC 404 equipped with a platinum furnace and a platinum/rhodium sample carrier was used for the measurements. TG analyses of specimens were carried out using a Netzsch STA 409 in an atmosphere of static argon, oxygen and air at heating rates from 3 to 10 °C min^{-1}. Because of the use of single crystals, a large contact area between the flat surface of the samples studied and the platinum crucible was possible.

Three scans on the DSC 404 were required in order to obtain the necessary experimental data to calculate the specific heat. The first scan is an empty sample pan run to establish a baseline; the second is a sapphire standard run to assess the sensitivity; and the third scan is a sample run. All experiments on the DSC 404 instrument are conducted at a heating rate of 20 °C min^{-1} from 50 to 950 °C.

The temperature control of the DSC 404 and the STA 409 was provided by a Netzsch 413 programmer and 413 controller. Data acquisition and instrument control were provided by a computer system with peripheral units and appropriate software.

X-ray diffraction patterns of the samples were obtained using a Geigerflex X-ray diffractometer with Cu K_α radiation as the X-ray source.

RESULTS AND DISCUSSION

The specific heat curves of $Bi_{12}SiO_{20}$ and $Bi_{12}GeO_{20}$ are shown in Fig. 1. The $C_p(T)$ obtained is different for specimens from different crystals. It

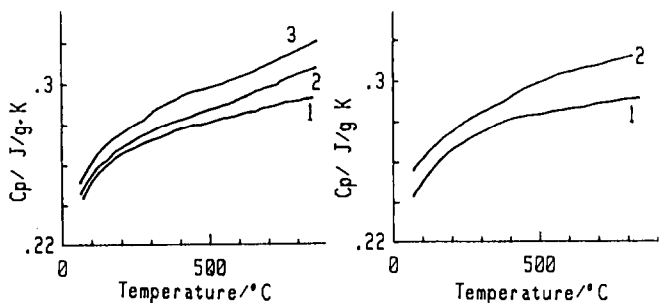

Fig. 1. The specific heat of single crystal samples: (left), $Bi_{12}GeO_{20}$: 1, crystal 1; 2, crystal 2; 3, crystal 3; (right), $Bi_{12}SiO_{20}$: 1, crystal 1; 2, crystal 2.

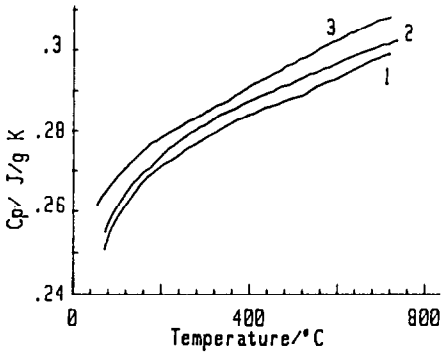

Fig. 2. Specific heat curves of: 1, $Bi_{38}ZnO_{58}$; 2, $Bi_{25}GaO_{39}$; and 3, $Bi_{25}FeO_{39}$.

should be noted that in order to avoid accidental errors, measurements were made for two different specimens in each crystal, the results of which agreed well.

A great deal of effort has been devoted to explaining the scattering of the $C_p(T)$ curves. From studying the crystal growth technique, it was assumed that slight variations in composition due to deviations in the starting oxide ratio affect the specific heat values of the crystals. This assumption will be discussed in this paper.

The specific heat curves for $Bi_{12}(M_{1-x}Bi_x)O_{20-y}$(M = Fe, Ga, Zn) are shown in Fig. 2. The specific heat curves approximated by polynomic equations are presented in Table 2, together with melting enthalpies and the melting or decomposition temperatures obtained in the present research.

Figure 3 shows the heat capacity curves obtained for bismuth gallate, zincate and titanate, together with the heat capacity curves of two samples of bismuth germanate. The heat capacity values were calculated per mole of $Bi_{12}(M_{1-x}Bi_x)O_{20-y}$, using the crystallochemical formulae given in Table

TABLE 2
The specific heat values approximated by the equation $C_p(\pm t_{0.05}s_0) = a + bT + cT^2 + dT^3$ ($J\,g^{-1}\,K^{-1}$)

	$a\times10^{-3}$	$b\times10^{4}$	$c\times10^{7}$	$d\times10^{10}$	$t_{0.05}s_0$
$Bi_{12}GeO_{20}$,max	130.8± 6.2	5.39±0.29	6.17±0.42	2.58±0.19	2.4
$Bi_{12}GeO_{20}$,min	142.4± 8.0	4.54±0.37	5.12±0.54	2.03±0.25	3.0
$Bi_{12}SiO_{20}$,max	213.9± 8.7	1.50±0.41	0.41±0.62	0.12±0.29	3.0
$Bi_{12}SiO_{20}$,min	99.1± 8.7	6.47±0.40	7.64±0.58	3.07±0.27	3.2
$Bi_{12}TiO_{20}$	181±11	3.13±0.56	3.14±0.88	1.24±0.44	3.0
$Bi_{12}(Bi_{0.5}Ga_{0.5})O_{19.5}$	165±12	3.46±0.62	3.61±0.96	1.41±0.47	3.6
$Bi_{12}(Bi_{0.5}Fe_{0.5})O_{19.5}$	171±12	3.35±0.61	3.52±0.94	1.38±0.47	3.6
$Bi_{12}(Bi_{0.67}Zn_{0.33})O_{19.33}$	160±14	3.90±0.71	4.8 ±1.1	2.10±0.56	3.8

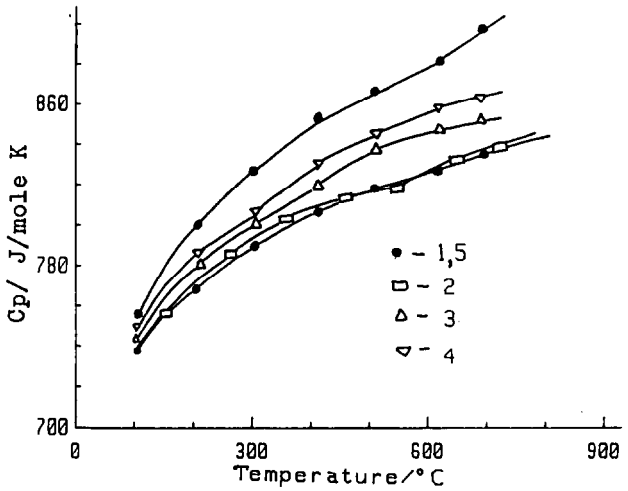

Fig. 3. Heat capacity values calculated per mole of $Bi_{12-y}(M_{1-x})O_{20}$: 1.5, $Bi_{12}GeO_{20}$; 2, $Bi_{12}(Bi_{0.67}Zn_{0.33})O_{19.33}$; 3, $Bi_{12}(Bi_{0.5}Ga_{0.5})O_{19.5}$; 4, $Bi_{12}TiO_{20}$.

1. The analysis of the data obtained was rather complicated. It was therefore necessary to supplement the heat capacity data with structural and electrophysical properties. As seen from Table 1, the increase in the unit cell parameters associated with crystal lattice changes and the decrease in thermal stability from $Bi_{12}GeO_{20}$ to $Bi_{38}ZnO_{58}$, are accompanied by a change in the melting character, from congruent melting for $Bi_{12}GeO_{20}$ and $Bi_{12}SiO_{20}$ to incongruent melting for the other compounds considered.

Therefore, we propose that the lattice contribution in the heat capacity of $Bi_{12}GeO_{20}$ and $Bi_{12}SiO_{20}$ is smaller than that of the other crystals, and that the specific heat values are higher for crystals with lattice distortion caused by interaction of the lattice with the tetrahedral cation (M or Bi). At least, the lattice contribution in C_p for all sillenite-type crystals was not expected to differ noticeably.

Because the real $C_p(T)$ curves of $Bi_{12}GeO_{20}$ and $Bi_{12}SiO_{20}$ are scattered over a wide range, there is clear evidence of some additional contributions to the specific heat. This is concluded from the present thermochemical study of samples treated under various thermodynamic conditions ($P(O_2)$, T).

The thermochemical properties of the compounds studied may be interpreted on the basis of a knowledge of the defect structure. As shown in Fig. 4, heating sample A of $Bi_{12}GeO_{20}$ at 440 °C in argon for 3.5 h and heating sample O in oxygen for 10 h, resulted in overlapping $C_p(T)$ curves. The result obtained confirms the correlation between the specific heat value and the changes that occurred in the oxygen sub-lattice, and the oxygen loss was assumed to induce the increase in C_p. In ref. 4, the heating of

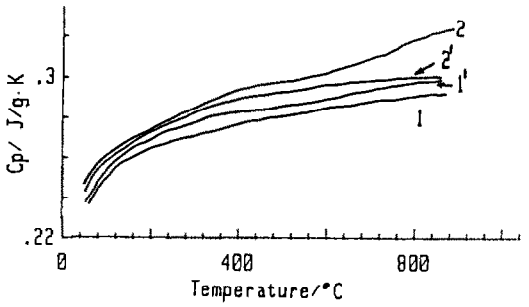

Fig. 4. Specific heat of $Bi_{12}GeO_{20}$: sample A: 1, primary curve; 1', curve after argon treatment; sample O: 2, primary curve, 2', curve after oxygen treatment.

$Bi_{12}GeO_{20}$ single-crystal specimens in atmospheres with different oxygen partial pressures resulted in reversible changes of the photocurrent by two orders of magnitude. A correlation is, in fact, observed between the specific heat behaviour in the present work and the changes in photoconductive properties and thermally stimulated current induced by an appropriate treatment reported in ref. 4.

It seems reasonable to propose that the increase in photoconductivity induced by thermal excitation of deep electronic levels, raises the electronic contribution in the specific heat. It is also necessary to take into account the configurative contribution to the specific heat arising from a statistical disorder caused by the point defects of the crystals.

The conclusions obtained may be represented by the results of studies on pure bismuth titanate crystals grown from different starting mixtures (6 and 8 mol.% TiO_2), and on single crystals doped with vanadium and zinc. The magnitudes of the specific heat of both pure crystals are in close agreement, as these specimens, evidently, have the same deviations from stoichiometric composition and, consequently, equal concentrations of titanium and oxygen vacancies.

The heat capacity values, compared to those of bismuth germanate, are shown in Fig. 3. The lowest $C_p(T)$ curve of $Bi_{12}GeO_{20}$ represents the total heat capacity curve, in which all contributions may be very small compared with the lattice contribution. Assuming that the lattice contributions for isomorphous compounds are close, the heat capacity of bismuth titanate may be considered to comprise the electronic and configurative contributions as well as the lattice contribution.

According to refs. 11 and 12, in the case of 0.15 wt.% vanadium doping, the photoconductivity increases by several orders of magnitude, whereas 0.1 wt.%, zinc doping reduces the photoconductivity. The specific heat variations for pure and doped crystals (see Fig. 5) correlate with the photoconductivity changes caused by doping.

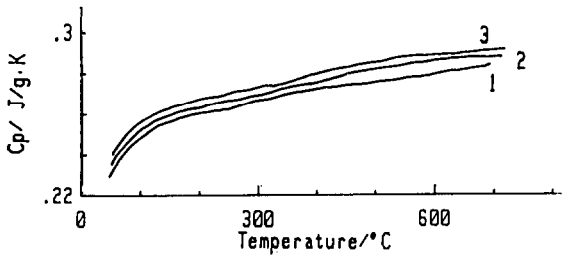

Fig. 5. Specific heat curves: 1, $Bi_{12}TiO_{20}$ doped with Zn; 2, pure $Bi_{12}TiO_{20}$; 3, $Bi_{12}TiO_{20}$ doped with V.

The additional heating of sample A of $Bi_{12}GeO_{20}$ in argon at 440 °C for 7 h did not result in the specific heat of sample O (curve 2, Fig. 4): on the contrary, it led to a fall in the specific heat.

It is, therefore, of interest to clarify the nature of the phenomena taking place in bismuth-containing oxides in an oxygen-deficient atmosphere. In the present research, it was observed that metallic bismuth condensed in a cooling zone of the silica tube whilst sillenite-type crystal specimens were being heated in a dynamic vacuum ($P_{O_2} = 10^{-5}$ atm) within the range 400–600 °C. The thermally activated evaporation of bismuth from the crystal lattice resulted from the high value of the bismuth vapour pressure and the low melting temperature of bismuth ($t_m = 271$ °C), and could be accelerated by oxygen deficiency in the crystal lattice. These phenomena are complex; the kinetics of the process was found to depend on temperature and to have a complex non-monotonous character [4].

There was no intention to study these phenomena, as more specific research is necessary to solve this problem. However, to prevent bismuth loss, an appropriate temperature for the isothermal heating has to be chosen. Nevertheless, at 440 °C this process obviously took place with extended heatings and resulted in a decrease in the specific heat.

With the reasonable assumption that bismuth loss implies an increase in the Ge–Bi ratio, the result was agreement with the authors of ref. 4 on the effect of the photocurrent elimination as a consequence of the increase in the germanium content.

The metastable phase inclusion

Figure 6 shows the plot of the specific heat for a $Bi_{25}GaO_{39}$ crystal specimen. The $C_p(T)$ curve shows an exothermal effect at 250–350 °C without any changes in the TG. Such a thermal effect has been recorded in the DSC curves of only a few crystals of bismuth zincate, ferrate and gallate, and this is the largest. According to refs. 13, DTA curves of the metastable δ*-phase of Bi_2O_3 doped with GeO_2 showed a similar exothermic peak corresponding to the phase transition in the γ-phase.

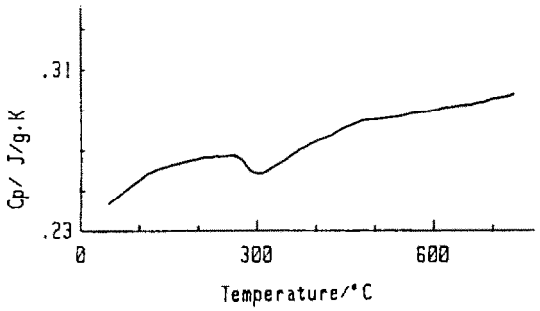

Fig. 6. Specific heat of $Bi_{25}GaO_{39}$ with δ^*-Bi_2O_3 inclusion.

The occurrence of the metastable δ^*-phase in Bi_2O_3–MO_2 systems has been established [14]. The δ^*-phase should be considered as a solution for small amounts of metal oxide in the high-temperature δ-phase of Bi_2O_3. Since single crystals are grown from the melt, they may contain inclusions of metastable δ^*-Bi_2O_3, caused by overheating of the melt. Therefore, the heat released was attributed to the conversion of δ^*-phase to γ-phase, the transition temperature of which is believed to depend on the heating rate; the temperature range of 250–350 °C for the heating rate of 20 °C min^{-1} agreed with our results.

The inclusion of the metastable phase may be a result of excess Bi_2O_3 in the starting mixture, according to the crystal growth technique from the solution in the melt. These inclusions could be expected to be eliminated by using the hydrothermal crystal growth technique.

CONCLUSION

DSC calorimetry was used for studying optically active sillenite-type single crystals. It was shown that the electronic contribution in the specific heat arose from the thermal stimulation of the electronic levels, associated with the point defects of the crystal. The contribution proceeding from the statistical disorder of the point defects accompanied the electronic contribution.

Because the defect structure depends on the composition, both the increase in the Bi–Ge ratio and the oxygen loss result in an increase in the specific heat. The same correlation was assumed for $Bi_{12}SiO_{20}$ single crystals.

For bismuth titanate, the changes in the specific heat arising from doping effects, were clarified.

Bismuth gallate, ferrate and zincate crystals tended to have metastable phase inclusions, presumably resulting from the use of the crystal growth technique from the solutions in the molten phase.

ACKNOWLEDGEMENTS

The authors thank Dr. V.V. Volkov for providing them with the single crystals for study, and Dr. Yu.F. Kargin for valuable discussion.

REFERENCES

1 E.M. Levin and R.S. Roth, J. Res. Natl. Bur. Stand. Sect. A, 68 (1964) 189.
2 H.A. Harvig and A.G. Gerards, Thermochim. Acta, 28 (1979) 121.
3 B.C. Grabmaier and R. Oberschmid, Phys. Status Solidi A, 96 (1986) 199.
4 O.A. Gudaev, V.A. Detinenko and V.K. Malinovski, Russ. Solid State Phys., 23 (1981) 195.
5 Yu. Berezovskaya, S. Budurov and T. Spasov, Cryst. Res. Technol., 22 (1987) 1421.
6 Yu. Berezovskaya, S. Budurov and T. Spasov, Cryst. Res. Technol., 22 (1987) 1415.
7 S.C. Abrahams, P.B. Jamieson and J.L. Bernstein, J. Chem. Phys., 47 (1967) 4034.
8 S.F. Radaev, L.A. Muradyan, Yu. F. Kargin, V.A. Sarin and V.I. Simonov, Proc. 12th Eur. Crystallographic Meeting, USSR, Moscow, 1989, Vd. 2, p. 138.
9 S.F. Radaev, PhD thesis, Moscow, USSR, 1989.
10 S.L. Hou, R.B. Lauer and R.E. Aldrich, J. Appl. Phys., 44 (1973) 2652.
11 V.M. Skorikov, V.I. Chmirev, N.A. Chumaevski, M.A. Baisimakov and V.V. Volkov, Russ. Vysokochist. Veshestva, 1 (1990) 218.
12 V.M. Skorikov, V.I. Chmirev, M.A. Baisimakov, V.V. Volkov and Yu.F. Kargin, Izv. Acad. Sci. USSR, Ser. Neorgan. Mater., 24 (1988) 1869.
13 P. Davidson, F. Marsaud, J.P. Bonnet and J.C. Launau, Chem. Scr., 27 (1987) 407.
14 I.V. Tananaev, V.M. Skorikov, Yu.F. Kargin and V.P. Jereb, Izv. Acad. Sci. USSR, Ser. Neorgan. Mater., 14 (1978) 2029.